3-Dimensional thermal analysis and active cooling of short-length high-power fiber lasers

L. Li, H. Li, T. Qiu, V. L. Temyanko, M. M. Morrell, and A. Schülzgen

Optical Sciences Center, the University of Arizona, Tucson, AZ 85721
lli@email.arizona.edu

A. Mafi and J. V. Moloney

Arizona Center for Mathematical Sciences, the University of Arizona, Tucson, AZ 85721

N. Peyghambarian

Optical Sciences Center, the University of Arizona, Tucson, AZ 85721

Abstract: A fully 3-dimensional finite element model has been developed that simulates the internal temperature distribution of short-length high-power fiber lasers. We have validated the numerical model by building a short, cladding-pumped, Er-Yb-codoped fiber laser and measuring the core temperature during laser operation. A dual-end-pumped, actively cooled, fiber laser has generated >11 W CW output power at 1535 nm from only 11.9 cm of active fiber. Simulations indicate power-scaling possibilities with improved fiber and cooling designs.

OCIS codes: (140.3510) Lasers, fiber; (060.2410) Fibers, erbium.

References and links

1. Y. Wang, "Thermal effects in kilowatt fiber lasers," IEEE Photon. Tech. Lett. **16**, 63-65 (2004).
2. Y. Jeong, J. K. Sahu, D. N. Payne, and J. Nilsson, "Ytterbium-doped large-core fibre laser with 1 Kw of continuous-wave output power," Electron. Lett. **40**, 470- 471 (2004).
3. P. K. Cheo and G. G. King, "Clad-pumped Yb:Er codoped fiber lasers," IEEE Photon. Tech. Lett. **13**, 188- 190 (2001).
4. J. Nilsson, S. Alam, J. A. Alvarez-Chavez, P. W. Turner, W.A. Clarkson, and A. B. Grudinin, "High-power and tunable operation of erbium-ytterbium co-doped cladding-pumped fiber lasers," IEEE J. Quantum Electron. **39**, 987-994 (2003).
5. J. K Sahu, Y. Jeong, D. J. Richardson, and J. Nilsson, "A 103 W erbium-ytterbium co-doped large-core fiber laser," Opt. Commun. **227**, 159-163 (2003).
6. C. Spiegelberg, J. Geng, Y. Hu, Y. Kaneda, S. Jiang, and N. Peyghambarian, "Low-noise narrow-linewidth fiber laser at 1550 nm," J. Lightwave Tech. **22**, 57-62 (2004).
7. L. Li, M. M. Morrell, T. Qiu, V. L. Temyanko, A. Schülzgen, A. Mafi, D. Kouznetsov, J. V. Moloney, T. Luo, S. Jiang, and N. Peyghambarian, "Short cladding-pumped Er/Yb phosphate fiber laser with 1.5 W output power," Appl. Phys. Lett. **85**, 2721-2723 (2004).
8. T. Qiu, L. Li, A. Schülzgen, V. L. Temyanko, T. Luo, S. Jiang, A. Mafi, J. V. Moloney, and N. Peyghambarian, "Generation of 9.3-W multimode and 4-W single-mode output from 7-cm short fiber lasers," IEEE Photon. Technol. Lett. **16**, 2592-2594 (2004).
9. D. C. Hanna, M. J. McCarthy, and P. J. Suni, "Thermal considerations in longitudinally pumped fibre and miniature bulk lasers," in *Fiber laser sources and amplifiers*, M. J. F. Digonnet, eds., Proc. SPIE **1171**, 160-166 (1989).
10. L. Zenteno, "High-power double-clad fiber lasers," J. Lightwave Tech. **11**, 1435-1446 (1993).
11. D. C. Brown and H. J. Hoffman, "Thermal, stress, and thermo-optic effects in high average power double-clad silica fiber lasers," IEEE J. Quantum Electron. **37**, 207-217 (2001).
12. J. Limpert, T. Schreiber, A. Liem, S. Nolte, H. Zellmer, T. Peschel, V. Guyenot, A. Tünnermann, "Thermal-optical properties of air-clad photonic crystal fiber lasers in high power operation," Opt. Express **11**, 2982-2990 (2003).
13. Y. Huo and P. K. Cheo, "Thermomechanical properties of high-power and high-energy Yb-doped silica fiber lasers," IEEE Photon. Technol. Lett. **16**, 759-761 (2004).
14. Finite element software ANSYS 6.1, http://www.ansys.com/

#6826 - $15.00 US Received 10 March 2005; revised 20 April 2005; accepted 20 April 2005

15. M. D. Shinn, E. A. Sibley, M. G. Drexhage, and R. N. Brown, "Optical transitions of Er^{3+} ions in fluorozirconate glass," Phys. Rev. B. **27**, 6635-6648 (1983).
16. H. Berthou and C. K. Jörgensen, "Optical-fiber temperature sensor based on upconversion-excited fluorescence," Opt. Lett. **15**, 1100-1102 (1990).
17. J. P. Holman, *Heat Transfer*, (McGraw-Hill Book Company, New York, 1986), Appendix A.
18. S. Jiang, M. Myers, and N. Peyghambarian, "Er^{3+} doped phosphate glasses and lasers," J. Non-Cryst Solids **239**, 143-148 (1998).

1. Introduction

Thermal problems have been of little concern to high-power cladding-pumped fiber lasers, especially the Yb^{3+}-doped silica fiber lasers at ~1.1 μm. Many factors contribute to the reduced importance of the thermal issue in this case: fibers have inherently large surface-to-volume ratios; thermal loads are usually spread over meters or tens of meters of fibers; cladding-pumping schemes effectively reduce the pump absorption coefficient; Yb^{3+}-doped lasers at ~1.1 μm have high quantum efficiencies (up to 90% if pumped at ~980 nm); and silica has a high transition temperature (>1000ºC). Yb^{3+}-doped fiber lasers have been predicted [1] and demonstrated [2] to generate CW optical power beyond 1 kW from a single fiber. The reported kW fiber laser had an average thermal load of ~35 W/m and operated without special cooling arrangements [2]. While heat hasn't been an issue for fiber lasers at ~1.1 μm, it is an issue for Er^{3+}-doped fiber lasers at the important eye-safe telecom wavelength ~1.5 μm. The quantum efficiency of these fiber lasers is limited to ~60% if pumped at ~980 nm. This results in more heat generation compared with that of the Yb^{3+}-doped fiber lasers. Cladding-pumped Er-Yb-codoped fiber lasers (EYDFLs), which are the most common fiber sources to generate high-power 1.5 μm signals, usually require meter-long active fibers to generate watt-level CW output powers [3-5]. For the highest reported output power of ~100 W from a single fiber, the average thermal load was ~20 W/m and the fiber wasn't actively cooled except at the pump power launching end [5].

Heat becomes a serious concern when high power 1.5 μm signal is generated from a very short fiber cavity, such as the recently reported short EYDFLs with watt-level CW output powers from active fibers only a few centimeters long [6-8]. With an average thermal load approaching ~200 W/m, passive cooling is insufficient to remove the excessive heat and active (forced) cooling becomes a necessity, e.g., the short EYDFLs capable of delivering ~9 W CW output power became possible only after they were actively cooled by water [8]. Considering the heavy thermal load of short EYDFLs, plus the fact that these fibers are made of phosphate glasses with a much lower glass transition temperature (T_g = ~600ºC) than silica, the heat removal capability may become the limiting factor for power scaling. Although the water-cooling scheme has been proven to be effective, it is preferable to cool the EYDFL in a solid-state method, e.g., by a thermoelectric cooler (TEC), for the benefits of compact device integration, simplified fabrication process, and easier operation.

Thermal analysis is an extremely important issue for these short high-power fiber lasers. To calculate the internal temperature distribution of fiber lasers, analytical solutions have been obtained for fibers with simple cylindrical symmetry [9-11], while numerical methods have been applied to the more complicated microstructured and multicore fibers [12,13]. These numerical calculations have all been performed in a 2-D frame, ignoring any longitudinal variation by averaging the thermal load over the fiber length. The averaged 2-D simulations for long fibers with small pump absorption coefficients constitute reasonable approximation to reality. However, this is not the case for end-pumped short EYDFLs, where the thermal load has a strong longitudinal dependence. On the other hand, the much shorter length of the active fibers, e.g., a few centimeters, made a full-length 3-D simulation feasible. Thus a 3-D thermal analysis is both necessary and possible for a short high-power fiber laser. Furthermore, although it is essential to verify the simulated fiber laser temperature, it is practically difficult to measure the internal temperature of a running fiber laser, which results in a noticeable lack of experimental verification for the fiber laser thermal simulation in literature.

#6826 - $15.00 US Received 10 March 2005; revised 20 April 2005; accepted 20 April 2005

In this paper, we report thermal analysis and practical construction of compact fiber laser assemblies that enable thermoelectric cooling. A fully 3-D finite element method (FEM) model [14] is built for the entire assembly to calculate its internal temperature distribution. To the best of our knowledge, going beyond standard cylindrical symmetry, this is the first comprehensive 3-D thermal analysis for fiber lasers with complex geometry. The heat source is formulated based upon detailed studies of the pump power absorption and heat conversion efficiency. Our thermal modeling is accompanied by measurement of the core temperature of a running EYDFL, which is, to the best of our knowledge, the first experimental attempt to obtain the internal temperature of a high-power fiber laser under operation. Both experiment and thermal analysis demonstrate that short TEC-cooled EYDFLs are capable of handling high-power laser action. An EYDFL, only 11.9 cm short, has been built and 11.1 W 1535 nm CW output power is obtained with combined 50.9 W 975 nm pump power launched onto dual ends. The thermal modeling is further employed to optimize the design of the active fiber and cooling setup, predicting that optimized TEC-cooled short EYDFLs have the capability to handle up to 200 W pump power, equivalent to a ~1 kW/m thermal load.

2. Single-end pumped TEC-cooled short EYDFL: 3-D FEM thermal modeling and experimental validation

The fiber studied here is a phosphate glass fiber heavily co-doped with 1.0 wt% Er_2O_3 and 8.0 wt% Yb_2O_3. The glass was provided by NP Photonics Inc. and the fiber was drawn at the Optical Science Center. The fiber has an off-center multimode core (D_{core} = 20±1 μm) and a D-shape cladding whose circular diameter is 130±2 μm. Both the D-shape cladding and off-center core are known to increase the pump absorption. In addition, the off-center core positioning can improve heat dissipation, as shown from our thermal analysis.

The TEC-cooled EYDFL assembly is shown in Fig. 1(a). A piece of active fiber, with both ends cleaved, is inserted into a borosilicate glass tubing whose inner diameter is slightly larger than the fiber. The glass tubing is cut exactly to the length of the fiber and the tubing is buried inside an aluminum (Al) block, which is attached to a TEC with 72 W heat removal capacity. An enlarged drawing of the fiber cross-section inside the tubing is shown in Fig. 1(b). The EYDFL assembly can be pumped through either end.

To demonstrate the feasibility of a TEC-cooling scheme under high power operation, we start with a relatively simple case of a single-end-pumped EYDFL in this section. We used the assembly outlined above, measured the core temperature during laser operation, and simulated the temperature distribution of the assembly using 3-D FEM modeling.

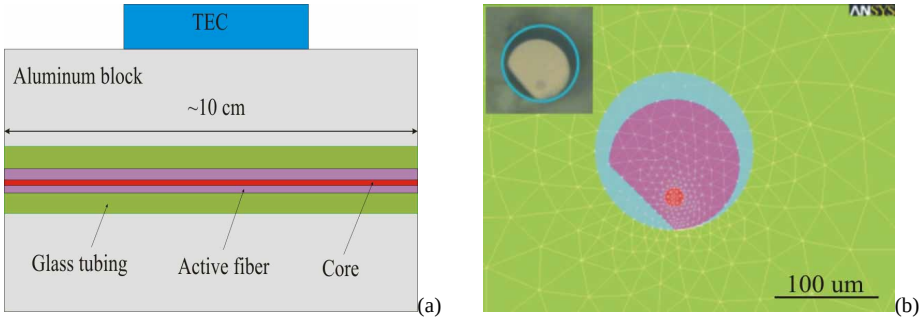

Fig. 1. The drawings of a TEC-cooled short-length EYDFL assembly: (a) the side view (fiber size not in proportion); (b) an enlarged end view with FEM meshes. The air gap in (b) (light blue) is not shown in (a) and the inset of (b) is a microscopic photo of the real fiber in tubing. The drawing (b) shows that the cladding (magenta) has a D-shape and the core (red) is in close proximity to heat sink-the glass tubing (green).

In the experiment, a 10.2-cm-long EYDFL was constructed and end-pumped through a multimode fiber, whose end was coated transparent to the pump light and highly reflective to the signal. The coated pump end was butt-coupled to the active fiber end so that the coating

#6826 - $15.00 US Received 10 March 2005; revised 20 April 2005; accepted 20 April 2005

served as the high reflector of the laser cavity. The other end of the active fiber was the output end. As the pump source, fiber-coupled multiple semiconductor laser diodes were used and their central wavelength was tuned to 975 nm, the Yb^{3+} absorption peak, by temperature control. The signal vs. absorbed pump power plot of the EYDFL is shown in Fig. 2(a). The EYDFL generated 7.5 W output power at 17.5 W absorbed pump power, corresponding to a 29.2 W launched pump power. To determine the absorbed pump power, we experimentally measured the pump coupling loss, scattering loss, and the pump leakage. The pump leakage was ~5% at low pump power and ~15% at high pump power. The laser slope efficiency with respect to the absorbed pump power (SE_{ABS}) was ~47%. The slope efficiency with respect to the launched pump power was ~25% over the full operation range and was only slightly affected by absorption saturation at the highest pump power.

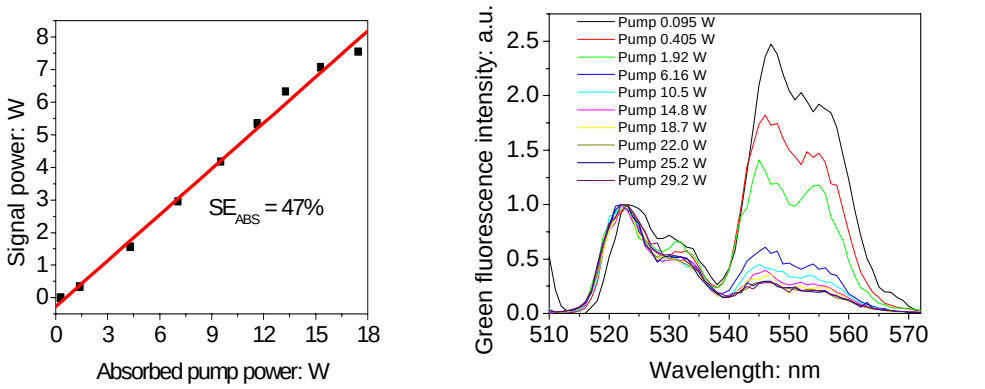

(a) (b)

Fig. 2. (a) The signal vs. absorbed pump power plot of a 10.2-cm long, single-end pumped EYDFL, the squares are measured data and the red line is a linear fit; (b) normalized spectra of Er^{3+} green UPF at different pump levels.

To measure the active core temperature, a piece of multimode fiber (core diameter of 100 μm) was brought to the close vicinity of the pump end to collect the Er^{3+} green upconversion fluorescence (UPF). The UPF collecting fiber was placed right at the pump power launching end and was oriented perpendicularly to the EYDFL axis. Thus only the UPF emitted from within a tiny cylindrical volume (< 100 μm from the pump end along EYDFL axis and 20 μm core diameter) was collected. The core temperature measured by this geometry was actually a volumetric average value, but it stood in good approximation to the highest temperature inside the core, as will be shown later by comparison with the simulation. The green UPF spectral shape has been known as a good temperature indicator for Er^{3+}-doped material [15,16]. The Er^{3+} UPF has two emission peaks located at ~523 and ~547 nm, resulting from $^2H_{11/2} \rightarrow {}^4I_{15/2}$ (I_H) and $^4S_{3/2} \rightarrow {}^4I_{15/2}$ (I_S) transitions, respectively. Assuming that $^2H_{11/2}$ and $^4S_{3/2}$ energy levels are in thermal equilibrium, the two emission intensities satisfy the following relation [15]:

$$\frac{I_H}{I_S} = C_T \exp\left(-\frac{\Delta E_{HS}}{K_B T}\right) \tag{1}$$

where ΔE_{HS} is the energy gap between the two levels, K_B is the Boltzmann constant, T is the temperature of the emitting material, and C_T is a constant that was determined by calibration. The green UPF was detected by a Hamamatsu H957-01 photo multiplier tube through a SPEX 270M monochromator. The normalized fluorescent spectra at different pump powers are shown in Fig. 2(b). The change in relative emission intensity is clearly observed and the deduced core temperatures are plotted with respect to the launched pump power as the red diamonds in Fig. 3. We observe a nonlinear dependence of the temperature with increased pump power, which will be explained by a nonlinear pump absorption coefficient discussed

#6826 - $15.00 US Received 10 March 2005; revised 20 April 2005; accepted 20 April 2005

later. Please note that such a real-time temperature monitoring of running high-power fiber lasers hasn't been reported in literature, and its realization certainly will provide important thermal information that otherwise could only be approached by simulation.

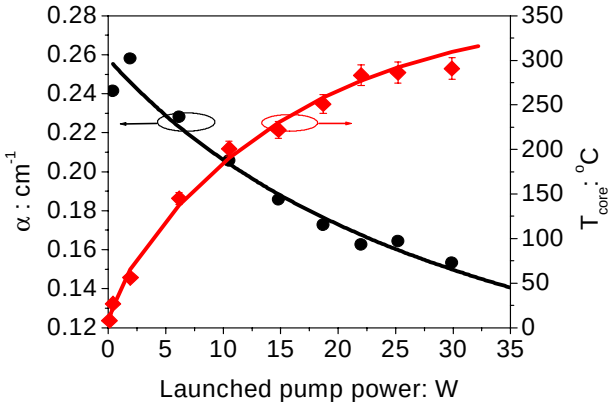

Fig. 3. Left Y-axis: the effective pump absorption coefficient α at different pump powers, the dots are the measured data and the line is fitted with formula $\alpha = \alpha_{SCT} + \alpha^{0}_{ABS} /(1+P/P_S)$. Right Y-axis: the highest core temperature at the pump end of a single-end-pumped EYDFL, the diamonds are measured data and the curve is the 3-D FEM simulated result.

To calculate the internal temperature distribution of the short EYDFL under forced cooling, we first establish the 3-D steady-state heat conduction equation inside the assembly:

$$\nabla\bullet[k(\boldsymbol{r},\mathrm{T})\nabla\mathrm{T}(\boldsymbol{r})] = -q(\boldsymbol{r}) \tag{2}$$

where $\boldsymbol{r} = \boldsymbol{r}(\mathrm{X}, \mathrm{Y}, \mathrm{Z})$ is the 3-D position vector, $k(\boldsymbol{r}, \mathrm{T})$ is the temperature-dependent local thermal conductivity, $\mathrm{T}(\boldsymbol{r})$ is the local temperature, $\nabla\,\mathrm{T}(\boldsymbol{r})$ is the temperature gradient, and $q(\boldsymbol{r})$ is the volumetric heat generation rate. Because conduction is the dominant heat transfer process under forced cooling in our setup, we neglect all other transfer processes such as convection and radiation in our calculation. The internal temperature distribution $\mathrm{T}(\boldsymbol{r})$ can be obtained by solving equation (2), accounting for heat fluxes in both radial and axial (Z) directions. The boundary condition of equation (2) is decided by the method of cooling (TEC-cooling in our case).

To numerically solve equation (2), a 3-D FEM model [14] for the EYDFL assembly was built, which included 3-D models of the active fiber and the cooling components. SOLID90 [14], a second order 3-D 20-node thermal element, was used to mesh the entire fiber laser assembly. A 2-D finite element mesh was generated first for the cross-section of the assembly, and then extruded in Z direction to build the fully 3-D finite element mesh. Various mesh sizes were used at different portions of the assembly, with smaller mesh sizes used at the pump power launching end. Because of the high heat flux over this region, especially at the radial direction (the forced cooling direction), the minimal node spacing used along the radial direction was less than 2 μm. The node spacing used along Z direction was 200 μm. The much smaller heat flux and temperature variation along Z make it unnecessary to further divide the mesh, and it would also be beyond the computational capacity of our FEM software if we use a micrometer-level division along the extended Z direction (~10 cm). An enlarged 2-D drawing of the cross-section of our FEM model is shown in Fig. 1(b). It highlights the position of the active fiber and its core inside the tubing, and also shows the arrangement of the FEM meshes. A minimal air gap was left between the fiber and the tubing inner wall due to the size mismatch. The air gap was necessary to allow for fiber insertion, but was found to be one of the critical factors limiting efficient heat dissipation.

The thermal conductivities of Al, borosilicate glass, and phosphate glass were chosen to be 190 [17], 1.14 [17], and 0.85 W/(m·K) [18], respectively, and were assumed temperature

#6826 - $15.00 US Received 10 March 2005; revised 20 April 2005; accepted 20 April 2005

independent. The thermal conductivity of air has a strong temperature dependence, which cannot be ignored, and values were chosen from Ref. 17. The temperature of the Al block was monitored during laser operation by a thermal couple embedded inside. Both the measurement and simulation showed that the maximal temperature difference across the Al block was less than 2°C. In our calculation, this difference was neglected and the measured temperature was used as the thermal boundary condition at the Al surface attached to the TEC. Adiabatic thermal boundary condition was applied to other part of the Al surface, due to the dominance of the TEC-forced cooling compared with any natural heat transfer processes.

An essential part in the thermal analysis is to correctly formulate the heat source. Instead of averaging the absorbed pump power (i.e. the thermal load) over the length, the heat source inside the active core was formulated under detailed study of the pump power propagation inside the core. Since our pump light was highly multimode, we assumed it had a flattop intensity distribution across the core area (no radial dependence). Thus the propagating pump power only had an exponential decaying Z dependence inside the active core:

$$P(Z) = P_0 \eta_C e^{-\alpha Z} \tag{3}$$

where P(Z) is the pump power at position Z, assuming that the initial pump power P_0 is coupled into the active fiber at Z = 0 with a coupling efficiency η_C = 85%. α is the effective pump absorption coefficient (a combination of the pump absorption coefficient α_{ABS} and the scattering coefficient α_{SCT}), which is a function of pump power. α was experimentally measured at different pump powers and fitted using the following formula:

$$\alpha = \alpha_{SCT} + \alpha_{ABS} = \alpha_{SCT} + \alpha^0_{ABS} / \left(1 + \frac{P}{P_S}\right) \tag{4}$$

Here α_{SCT} = 0.02 cm^{-1} is the pump scattering coefficient, assumed to be power independent; α^0_{ABS} = 0.24 cm^{-1} is the small-signal pump absorption coefficient. All η_C, $\alpha_{SCT,}$ and α^0_{ABS} were experimentally obtained by cutback measurements. P_S = 36.0 W is the saturation pump power obtained from data fitting in Fig. 3.

With the internal pump power distribution established, the heat (dQ) generated inside core at position Z with infinitesimal incremental length dZ can be formulated as:

$$dQ(Z) = \eta_{HEAT} \alpha_{ABS} P(Z) dZ \tag{5}$$

Assuming that all absorbed pump power is converted either to signal power or heat, the heat conversion efficiency η_{HEAT} is given by $\eta_{HEAT} = 1 - SE_{ABS}$, where SE_{ABS} can be calculated from the signal vs. absorbed pump power plot, e.g., SE_{ABS} = 47% in Fig. 2(a). The volumetric heat generation rate $q(\boldsymbol{r})$ in equation (2) can finally be determined from equation (5). Assume that $q(\boldsymbol{r})$ is zero everywhere except inside the active core. We also assume that $q(\boldsymbol{r})$ is constant across the core, reflecting the pump light intensity distribution. $q(\boldsymbol{r})$ is then given by:

$$q(\boldsymbol{r}) = q(Z) = \frac{1}{A}\frac{dQ}{dZ} \tag{6}$$

where A is the active core area.

Combining the heat source, thermal boundary conditions, material thermal properties, with the geometry and meshing shown in Fig 1(b), the 3-D FEM model was established and solved to obtain the temperature distribution inside the whole EYDFL assembly. The simulated highest temperatures (T_{max}) are plotted at different pump powers as the red curve in Fig. 3. T_{max} is located near the center of the core at longitudinal position Z = 0. The 3-D simulation shows that at all pump power levels, the temperature variation across the core area is less than 20°C. The longitudinal temperature variation along the cylindrical axis in the measurement is even smaller. At the same transversal coordinates, the temperature difference between positions at Z = 0 and Z = 200 μm (the second node along Z from Z = 0) is less than 2°C. Because the measured temperature was a volumetric average along and across the first

#6826 - $15.00 US Received 10 March 2005; revised 20 April 2005; accepted 20 April 2005

100 μm of the active core pumped, we concluded that the measured temperature should be within 10°C below the actual maximum temperature. Comparing the red curve with the red diamonds, we notice that the agreement between the measurement and simulation is very good. Please also note that our simulation and measurement have used completely independent approaches to obtain the temperature; the coincidence of their line shapes is excellent, which strongly confirms the validity of our 3-D thermal modeling. The thermal behavior of the emitting core is well explained by the nonlinear pump absorption coefficient curve in the same figure.

3. Optimized dual-end pumped short EYDFL: experimental improvement and 3-D FEM thermal optimization

The previous experiment demonstrates that our 3-D thermal modeling provides a good description of the internal temperature of the EYDFL assembly. As the next step, we build and analyze an advanced dual-end-pumped EYDFL. The dual-end-pumping scheme not only eases the thermal problem by splitting the pump power between both ends [1], but also provides more uniform gain along the length.

Comparing to the previous EYDFL, a second pump source was added onto the other fiber end and the active fiber was increased to 11.9 cm. Our thermal modeling predicted that it was thermally safe at ~50 W pump power. Thus a 50.9 W combined pump power (18.6 W at Z =0 and 32.3 W at Z = 11.9 cm) was launched and 11.1 W CW output power was obtained. The signal vs. launched pump power plot is shown in Fig. 4. To the best of our knowledge, this is the first 1.5 μm fiber laser capable of delivering beyond 10W CW output power with the length scale of a few centimeters. No sign of signal saturation was seen and the output power was only limited by the available pump power. Since the same active fiber was used, the laser performed similarly to that in Ref. 8. The spectrum was centered at 1535 nm with a 2-nm linewidth, and the measured M^2 value was < 4.0. There was no thermal damage at the two fiber ends up to the highest pump level, demonstrating that the TEC-cooled assembly adequately handled an average thermal load of ~180 W/m.

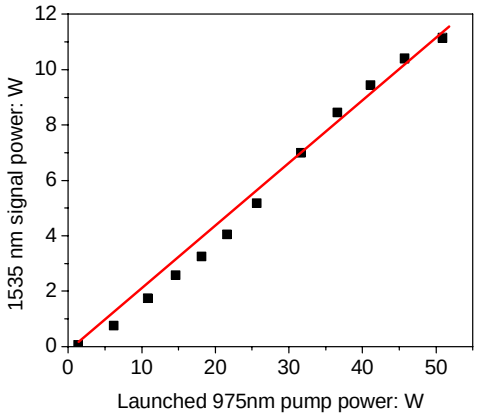

Fig. 4. The signal vs. launched pump power plot of the dual-end pumped EYDFL.

To simulate the dual-end pumped EYDFL, the pump power propagating inside core should be reformulated to include pump lights propagating along both +Z and –Z directions:

$$P(Z) = P_{0L}\eta_{CL}e^{-\alpha Z} + P_{0R}\eta_{CR}e^{-\alpha(L-Z)} \quad (7)$$

Here the left fiber end is placed at Z = 0; L is the fiber length; $P_{0L}$and P_{0R} are the launched pump powers on both ends, respectively; η_{CL} and η_{CR} are the pump coupling coefficients at the two fiber ends; α is treated the same as in equation (4).

#6826 - $15.00 US Received 10 March 2005; revised 20 April 2005; accepted 20 April 2005

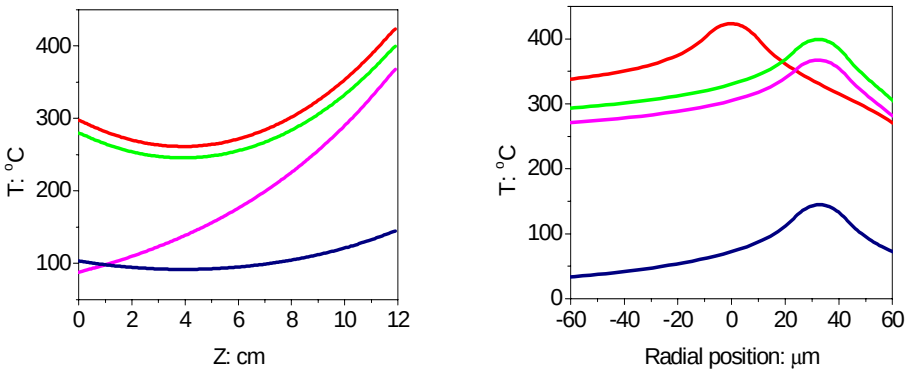

(a) (b)

Fig. 5. Temperature distributions in short TEC-cooled dual-end-pumped (except the magenta) EYDFLs: (a) core temperature along the fiber length; (b) temperature profile across the fiber facet at the stronger pump end. Green: simulations for the experimental configuration; magenta: single-end-pumped EYDFL; red: centered-core fiber; navy: double-cladding fiber in contact with Al heatsink.

In our 3-D FEM simulation, we placed the active fiber at the same position as in Fig. 1(b). The simulations for the tested design are plotted as the green curves in Fig. 5: 5(a) shows the core temperature along the fiber length and 5(b) shows the temperature profile across the fiber facet at the stronger pump power end. Although the calculated highest temperature (T_{max} = ~400ºC) reaches a substantial fraction of the phosphate glass transition temperature, the laser is still operational, as proven by the experiment. For comparison, the same calculation was done for a single-end-pumped EYDFL (pump power of 32.3 W launched on one end) and the results are plotted as the magenta curves in Fig. 5. We notice that T_{max} of the dual-end-pumped EYDFL was only 32ºC higher than that of the single-end-pumped one. Adding a second pump increased the output by ~50% but the T_{max} by only ~10%, a clear demonstration of the thermal advantage of dual-end pumping scheme. We also calculated the temperature distribution for a dual-end-pumped EYDFL with the active core in the circular center of D-shape cladding. The results are plotted as the red curves in Fig. 5. At the highest pump power, T_{max} increased by 24ºC, compared with our off-center-core design under otherwise identical conditions. This calculation demonstrates the thermal benefit of the off-center core that is closer to the heat sink.

Although our fiber laser assembly enabled operation up to ~50 W of pump power, it did not leave much room for further power scaling. As a next step, we used the 3-D FEM modeling as a powerful tool to guide further improvement in the thermal management of our short EYDFL assembly. Obviously the air gap is the largest obstacle to efficient heat dissipation. A double–cladding fiber structure with the same off-center core and a second 200-μm diameter circular cladding was considered, which allowed direct contact between the fiber and a metallic tubing (e.g., an Al tubing). Our calculation showed a significant temperature drop, as shown by the navy curves in Fig. 5. At the highest pump power, T_{max} dropped more than 250ºC to only 145ºC. This calculation demonstrates that heating problems can be solved even for a heavy thermal load within a small volume for optimized fiber and cooling setup. Our simulation shows that a short TEC-cooled fiber laser could handle a combined pump power of 200 W, corresponding to a thermal load of ~1 kW/m.

4. Conclusion

We demonstrated a 3-D FEM thermal analysis of short-length, actively cooled, high-power fiber lasers and experimentally verified the modeling results. Both simulation and experiment demonstrated the heat handling capability of the TEC-cooled EYDFLs. A dual-end-pumped EYDFL was built and more than 11 W CW optical power at 1535 nm was generated. The

#6826 - $15.00 US Received 10 March 2005; revised 20 April 2005; accepted 20 April 2005

thermal simulations further predicted that TEC-cooled fiber lasers have the potential to dissipate thermal loads up to ~1 kW/m.

Acknowledgments

The authors thank S. Jiang and T. Luo of NP Photonics Inc. for making the phosphate glasses, and E. Temyanko for coating the dielectric layers. This work is supported by the Air Force Office of Scientific Research through a MRI program No. F49620-02-1-0380 and the state of Arizona TRIF Photonics Initiative.

#6826 - $15.00 US Received 10 March 2005; revised 20 April 2005; accepted 20 April 2005